A Nonlethal Full-Thickness Flame Burn Produces a Seroma Beneath the Forming Eschar, Thereby Promoting *Pseudomonas aeruginosa* Sepsis in Mice

Jerod Brammer, PhD,[*,†] Gideon Wolf, BS,[†] Scott M. Baliban, PhD,[*] Jessica C. Allen, BS,[*,†] Myeongjin Choi, PhD,[*] Adrienne R. Kambouris, BS,[*,†] Raphael Simon, PhD,[*] Gary Fiskum, PhD,[‡] Wei Chao, MD, PhD,[‡] Kerri Lopez, MD,[‡,||] Catriona Miller, PhD,[§] Nevil J. Singh, PhD,[†] and Alan S. Cross, MD[*]

The World Health Organization estimates ~180,000 deaths occur annually from burn-related injuries. Many victims who survive the initial burn trauma succumb to bacterial infections that lead to sepsis during treatment. Although advancements in burn care continue to improve in high-income countries due to their burn centers and advanced research, low and middle-income countries continue to see high frequencies of burn injuries and burn-related deaths due to secondary infections. Bacterial-derived sepsis is the most life-threatening danger for people that survive burn injuries. Here we provide evidence for the first time that a subeschar seroma forms postburn even in the absence of infection in mice. The seroma fills with a volume estimated at 500 µL of fluid, 25% of the blood supply, free of red blood cells. The seroma fluid supports robust *Pseudomonas aeruginosa* (PA) growth and contains inflammatory cytokines and chemokines, which recruit immature neutrophils and monocytes to the seroma in the absence of endothelial breakdown. These immune cells fail to contain PA expansion and dissemination. This recruitment of monocytes and immature neutrophils may result in sequestering these critical immune cells away from other tissues during a pivotal time during bacterial dissemination, promoting PA-mediated sepsis.

According to the World Health Organization, an estimated 180,000 deaths occur each year from burns and burn-related injuries, while nonfatal burn injuries are a leading cause of morbidity and mortality due to tissue destruction and secondary infections.[1] For example, a 10-year retrospective study at the Erciyes University Burn Center in Turkey showed an 11% nosocomial infection rate of admitted burn patients with a median burn size of 10%.[2] Although casualty care of burn patients has dramatically improved over time and the current survival rate of people who reach a burn center in the United States of America is more than 95%, it is not the same for low to middle-income countries (LIC, MIC).[3,4] In comparison, LIC and MIC have 10 and 62 per 1,000,000 unintentional childhood deaths respectively from burn injuries, whereas in high-income countries (HIC), 1 in 1,000,000 children died from unintentional burn injuries each year.[3] One reason for these discrepancies is the level of care provided in HIC at dedicated burn centers, accredited by the American Burn Association (ABA). These burn centers provide admitted patients with wound care (ie, debridement, eschar excision, and grafting), resuscitation, stabilization, and rehabilitation.[5–7] Nonburn centers do not have the capabilities to support such procedures. Although debridement, eschar excision, and grafting are routine procedures in burn units, Soldiers who receive a significant thermal injury in combat do not have these procedures performed until they are evacuated from the combat zone to a burn center days after the initial injury. This delay in advanced care can lead to an increased risk of complications.[8]

A severe burn injury can lead to increased capillary permeability and a reduction in vascular volume. Fluid resuscitation is administered to supply organs with the required fluid.[5] However, fluid resuscitation has its challenges; if too much fluid is administered, the risk and likelihood of edema increase.[9] In rare cases, fluid from resuscitation in burned patients may collect between tissues within compartments, such as muscle tissue, leading to intracompartmental sepsis (IS).[10,11] Additionally, subeschar fluid has been shown to have immunological relevance and is capable of cell-mediated immune suppression.[12,13] In other traumas and surgeries, fluid can fill

*From the *Center for Vaccine Development and Global Health, University of Maryland, School of Medicine, Baltimore, USA; †Department of Microbiology and Immunology, University of Maryland, School of Medicine, Baltimore, USA; ‡Translational Research Program, Department of Anesthesiology & Center for Shock, Trauma and Anesthesiology Research, University of Maryland School of Medicine, Baltimore, USA; ||Department of Surgery, University of Maryland School of Medicine, Baltimore, USA; §Enroute Care Division, Department of Aeromedical Research, USAF School of Aerospace Medicine, Wright Patterson AFB, Dayton, Ohio, USA.*

Funding: This work was supported in part by a grant from the US Air Force Research (FA8650-18-2-6H17). The views expressed in this article are those of the authors and do not necessarily reflect the official policy or position of the Air Force, Army, the Department of Defense, or the U.S. Government.

Conflict of interest statement. None.

Address correspondence to Alan Cross, Center for Vaccine Development and Global Health, University of Maryland School of Medicine, 685 W Baltimore Street, Baltimore, MD 21201, USA. Email: across@som.umaryland.edu

https://doi.org/10.1093/jbcr/irab195

spaces between tissues and form seromas.[14] Seromas have been shown to support bacterial growth and colonization.[15] Here we present what we believe to be the first nonlethal mouse burn model that produced a seroma. A subcutaneous inoculation of <100 CFU of *Pseudomonas aeruginosa* (PA) strain M2 at the burn site immediately following the burn resulted in 100% mortality between 18 and 26 hours.[16] Thus, a nutrient-rich seroma was formed postburn that provided PA a reservoir for exponential growth and recruited immature neutrophils and monocytes, depleting them from the circulation and possibly from critical sites required to fight the PA infection seroma.

METHODS

Burn Procedure

Burns wounds were administered as previously described.[16,17] Female Crl:CD-1 mice (Charles River Laboratories, MA) between 6 and 10 weeks of age and weighing between 28 and 34 g Wahl™ clippers were used to remove the hair from the backs of each mouse 24 hours before the burn procedure. 5% isoflurane were used for 8 minutes to each mouse just before the burn. Adequate anesthesia was monitored by toe pinching. Mice were laid on their bellies in a chemical fume hood, a flame-resistant polymer card representing roughly 10% total body surface area (2.5 cm × 4.0 cm) was pressed down onto the back and 500 µL of 100% ethanol was deposited onto the surgical field with a pipet. The ethanol was ignited using a lighter, and a timer was used to ensure the burn lasted 10 seconds. The flame was extinguished by breath. Immediately postburn, mice were provided 500 µL intraperitoneally of Ringer's solution for fluid resuscitation. Mice were placed in their original housing cages and recovered on an HTP-1500 veterinarian-grade heating blanket (Adroit Medical Systems, Loudon, TN). Mice were infected directly after the burn with a subcutaneous injection of ~600 CFU PA M2 suspended in 100 µL of sterile saline. Sham mice received all treatment as test mice except for the burn and infection, unless otherwise stated.

Clinical Observations

Mice were checked twice daily, unless otherwise specified, and assigned a symptom score of 1 to 3 based on signs of distress.[18] At the onset of moribundity, mice were killed by either terminal anesthesia followed by cardiac puncture or CO_2 asphyxiation followed by cervical dislocation.

Terminal Blood Collection

Mice were placed under terminal anesthesia (5% isoflurane for 8 minutes). Sedation was assessed by toe pinch. Mice were placed on their backs, and the chest was sterilized with 70% ethanol. A 1 mL syringe with a 25 g needle was inserted into the heart. Whole blood was collected to a final volume between 500 and 1000 uL.

Seroma Pathology

Post-euthanasia, incisions were made through the eschar, which extended from the epidermis through the skeletal muscle and bone to reveal a 2 cm × 1 cm tissue sample that was placed into a tissue cassette and fixed in 10% formaldehyde for 3 days or encased in Histogel™ (Thermo Fisher Scientific). Samples were sectioned and stained for H&E staining, Gram-staining, or immunohistochemical (IHC) CD45+ staining at the University of Maryland School of Medicine (UMSOM) Center for Innovative Biomedical Resources (CIBR) Pathology Biorepository Shared Service. Slides were examined by a blinded pathologist and imaged at 600× magnification using a Keyence BZX all-in-one Microscope System (Keyence, Itasca, IL).

Bacterial Preparation

An ice chip from PA M2 glycerol stock was streaked for single colony isolates on Tryptic Soy Agar (TSA) (Sigma-Aldrich, St. Louis, MO) plates and incubated at 37°C for 18 hours. A single colony was transferred to 3.0 mL of Hy-Soy Broth, containing 0.5% sodium chloride (American Bio, Canton, MA), 0.5% HY-Yeast (Kerry Bio-Science, Norwich NY), and 0.25% animal-free soytone (Teknova, Hollister, CA) and grown to stationary phase at 37°C in a shaking incubator. Next, 1% volume was inoculated into 12 mL of Hy-Soy broth and grown at 37°C in a shaking incubator until mid-log-phase, OD600 of 0.6 to 0.8. The bacteria were pelleted, washed twice with sterile phosphate-buffered saline (PBS), and resuspended to the desired concentration.

Serum and Seroma Cytokine and Chemokine Analysis

IFN-γ, TNF-α, IL-1β, IL-6, and IL-10 along with IP-10, KC, MCP-1, MIP-1α, MIP-1β, and RANTES were measured in multiplex with the Luminex 100 reader in the UMSOM CIBR Cytokine Core Laboratory. All samples were run in duplicate and compared to internal controls.

Red Blood Cell Depletion

Whole blood was collected as previously described into heparin-coated tubes. Next, 400 µL of whole blood was transferred to a fluorescence-activated cell sorting (FACS) tube. Next, 500 µL of 1X FACS buffer (BSA, EDTA, sodium azide, and 10X PBS) was added and centrifuged at 1200 RPM for 7 min at 4°C. The supernatant was pipetted off and discarded. One mL of ammonium–chloride–potassium (ACK) lysis buffer was added and incubated at room temperature for 10 min. Cells were pelleted at 1200 RPM for 7 minutes at 4°C, the supernatant removed, and ACK lysis steps repeated. The remaining cells were resuspended in 500 mL of 1X FACS buffer and manually counted using a hemocytometer.

Collagenase Digestion

Seroma samples were placed into 50 mL conical tubes and incubated at 37°C for 2 hours with 2 mL of collagenase solution (2.5 g/mL collagenase D and 200 U/mL Dnase 1). Samples were pressed through a 70 µM cell strainer. Cells were pelleted at 1200 RPM for 7 min at 4°C, and the supernatant was removed. The remaining cells were resuspended in 500 mL of 1X FACS buffer and manually counted using a hemocytometer.

Flow Cytometry

Single-cell suspensions prepared by ACK lysis or collagenase digestion were centrifuged and resuspended in Fc-block

(a cocktail of mouse, rat, and hamster IgG, as well as anti-CD16/32 Rat anti-mouse IgG clone 2.4G2) for 15 minutes at 4°C. After this incubation, the primary antibodies were added to the cell suspension. The antibody panel used for these studies can be found in detail in Supplementary Table 1. Cells were incubated for 15 min with the antibodies at 4°C. Following this incubation, cells were washed, centrifuged, and resuspended in 500 µL 1X FACS buffer. Flow cytometry was performed using the Cytek Aurora flow cytometer (Cytek Biosciences, Fremont, CA), and analysis was performed using FlowJo (BD Biosciences).

Statistical Analysis

All statistics were performed on GraphPad Prism 7 and 9 (GraphPad Software La Jolla, CA). One-way ANOVA test with Tukey's multiple comparisons test was used to analyze cytokine and cell numbers over time, unless otherwise specified.

Ethics Statement

All animal work was performed at the UMSOM, which complies with guidelines for animal care established by the US Department of Agriculture Animal Welfare Act, US Public Health Services policies, and US federal law. All animal experiments were approved by the UMSOM Institutional Animal Care and Use Committee

RESULTS

A 10% TBSA Flame Burn Produced a Seroma Formation below the Forming Eschar

At 3 hours postburn (Hpb), mice were euthanized, and a traverse incision was made from the top of the eschar through the underlying skeletal muscle and bone to reveal a cross-sectional view. A fluidic layer was observed below the eschar but above the skeletal muscle. The fluid extended outside of the edges of the burn eschar (Figure 1A). The eschar was gently removed, using forceps and surgical scissors to reveal a transparent gelatinous formation separate from the skeletal muscle and the skin. The fluid layer appeared to replace the subcutaneous fascial plane and was easily manipulated with forceps (Figure 1B). When a deeper incision was made, an approximate 1 cm × 2 cm skin flap, which included the eschar and gelatinous fluid layer, was removed using forceps and scissors. Gentle scraping with a scalpel revealed an estimated 500 µL of completely transparent material with some veinous formations running through the seroma, although none terminated within the seroma (Figure 1C). These observations were made both with and without a subcutaneous infection with PA M2 immediately after the burn.

Seroma Fluid Originates from the Circulation

Our next goal was to observe the anatomical origins of the seroma fluid. Mice were injected with 20 mg FITC-dextran

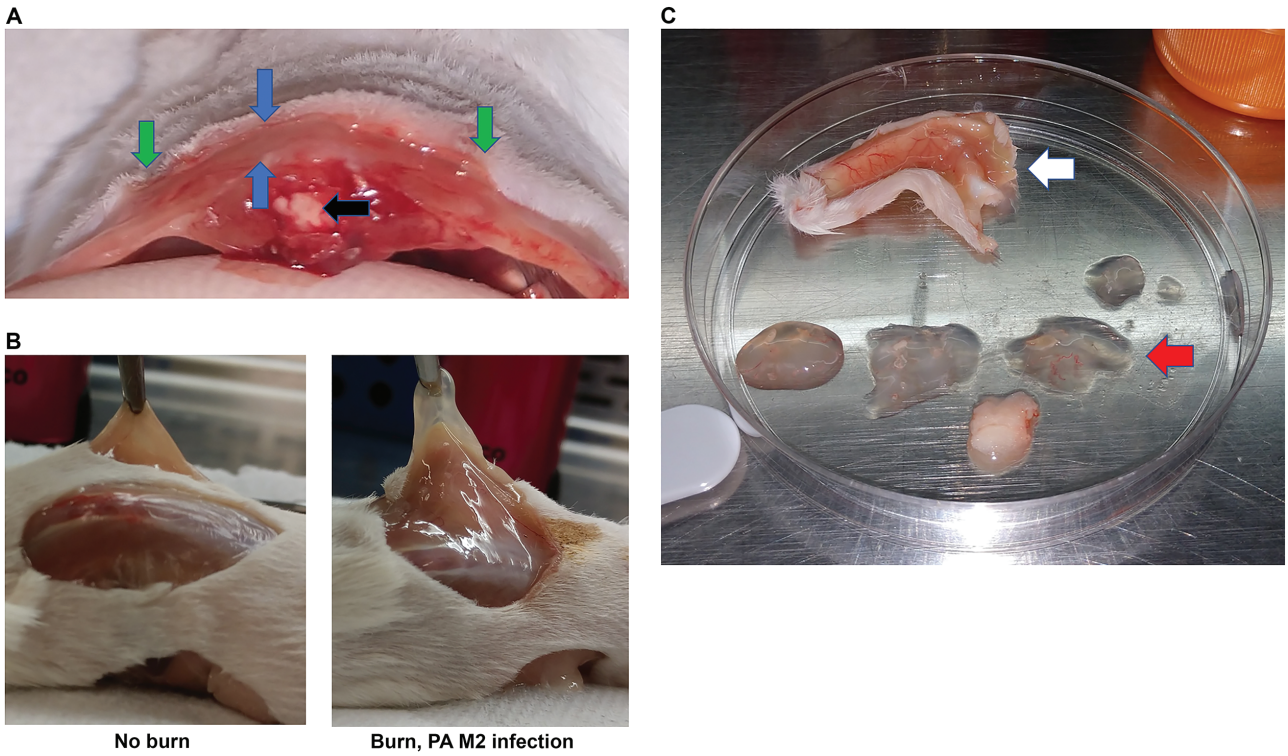

Figure 1. Gross observation of seroma formation under the forming eschar regardless of infection: (A) Three hours postburn (with or without infection), a gelatinous fluid layer built up under the burn site and protruded past the borders of the burn indicated by the green arrows. The blue arrows highlight the borders of the seroma layer. The black arrow designates the spine. (B) The seroma fluid forms in the fascia, which separates the skeletal muscle from the cutaneous layers. In nonburned mice, the fascia plane is a thin film overlaying the skeletal muscle. (C) A 1 cm × 2 cm skin flap of the eschar (white arrow) was removed; the seroma fluid (three clear zones marked by the red arrow came from the skin flap of one mouse) was removed by gently scraping with a scalpel.

4 kd intravenously (i.v.) 15 minutes prior to the burn. The (4 kd) size was chosen due to its small size and the likelihood of diffusion from the circulation to the seroma. The burn was administered 15 minutes post-i.v. injection of FITC-dextran. Seroma fluid was collected 3 Hpb without infection and assessed for FITC-dextran concentration. Burned mice that received i.v. FITC-dextran showed an average of 2.8 mg/g FITC-dextran in the seroma. (Supplementary Figure 1). The lack of seroma formation in unburned mice results in no appropriate control. These data show that the fluid in the seroma is derived primarily from the circulation.

Seroma Fluid Supports the Growth of *Pseudomonas aeruginosa* (PA) In Vitro

We previously reported that, PA infection is significantly more lethal following a 10% TBSA burn injury in mice.[17] Therefore, we hypothesized that the burn-induced seroma promotes the growth of PA. To test this, burned mice without infection were killed at 3 Hpb. Seroma fluid was harvested as described above, and 0.2 g suspended in 3 mL of PBS and homogenized. Four different strains of PA (925 CFU of PAO1(laboratory strain), 3600 CFU of SBI-N (IATS 06), 7000 CFU of PA14 (clinical isolate), and 650 CFU of PA M2 [intestinal isolate from a CF-1 mouse, IATS 05]) were inoculated into either seroma suspension or an equivalent volume of HySoy broth and incubated at 37°C with shaking. To assess bacterial growth, cultures were sampled every 2 hours to determine CFU/mL by serial dilution and plating on TSA agar. All four PA strains replicated at equivalent rates in the seroma suspension as they did in fortified bacterial culture media (Figure 2). The equivalent growth of PA strains in the seroma suspension compared to fortified growth media suggests that the seroma is a nutrient-rich environment that allows PA to grow to high concentrations locally before dissemination throughout the mouse.

Histology Showed a Short-lived Seroma Formation between the Panniculus Carnosus and the Skeletal Muscle/Adipose Tissue Originating below the Eschar

Mice were burned and killed at 3, 6, 12, and 18 Hpb. Deep, transverse incisions were made of the eschar that was immediately placed into 10% formalin for 72 hours. Observation of sham tissue sections showed a compact fascial plane (red arrow) between the panniculus carnosus and the underlying skeletal

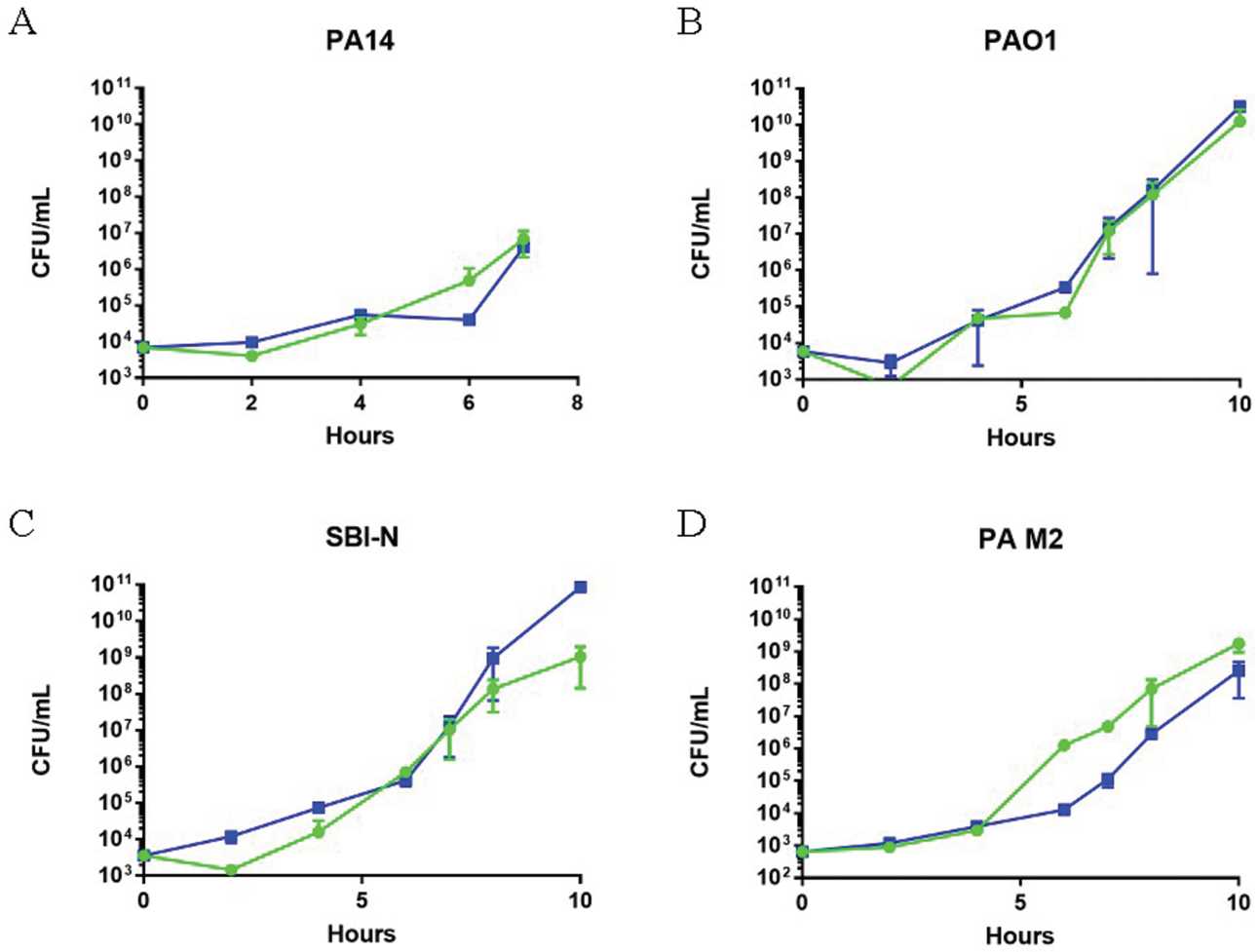

Figure 2. In vitro growth curve of different *Pseudomonas aeruginosa* strains in seroma suspension (squares) and fortified growth media (circles): PA strains (A) 7000 CFU of PA 14, (B) 925 CFU of PAO1, (C) 3600 CFU of SBI-N, and (D) 650 CFU of PA M2 were grown at 37°C on a shaker for 10 hours in either HySoy broth or seroma suspension. OD_{600} readings were taken every hour to determine bacterial growth.

muscle (blue arrow), ~57 µm in thickness (Figure 3A). By 3 Hpb, the panniculus carnosus and the skeletal muscle were separated by an influx of fluid with an average thickness of 1.18×10^3 µm. The fluid contained haphazardly-arranged collagenous material with rare fibroblasts and lymphocytes (Figure 3B). By 6 Hpb, the seroma could be seen extending beyond the burned border of the skin (black arrow) (Supplementary Figure 2). By 9 Hpb in the absence of infection, the seroma was 1.15 x 103 um in thickness, but by 12 Hpb it was reduced in thickness to ~567 um (Figures 3C and 3D respectively). However, a large influx of cells was observed throughout the seroma. The seroma was almost resolved at 18 Hpb (Figure 3E). The seroma was observed under two viable tissue layers, the subcutaneous adipose tissue and the panniculus carnosus. The subcutaneous adipose tissue and the panniculus carnosus were not damaged by the burn. Additionally, no apparent cellular breakdown of the panniculus carnosus or the underlying skeletal muscle/adipose tissue was observed, suggesting that the cellular infiltrates were actively recruited.

Seroma Contains Bacteria, Lymphocyte Infiltrates, and Cellular Necrosis

To characterize the composition of the seroma-fluid, samples were collected at 12 Hpb, using forceps and a scalpel from burned mice, with and without a subcutaneous infection with PA M2. We chose 12 Hpb based on our observation of robust cell infiltration (Figure 3D). A portion of the seroma was placed into Histogel™ and processed according to the manufacturer's protocol to be evaluated by pathologists for cell populations and tissue pathology. Without PA infection, the seroma showed edematous haphazard collagenous material, interpreted as collagen fibers and fibroblasts, with small mononuclear cells that appeared to be fibroblast nuclei and rare scattered lymphocytes (Figure 4A). With PA M2 infection, the appearance was similar, however the seroma contained increased numbers of leukocytes and cellular necrosis (Figure 4B); Further Gram stain analysis showed Gram-negative rods (GNRs) throughout the seroma and in proximity to granulocytes (Figure 4C). Immunohistochemical (IHC) CD 45+ staining of seroma from mice without PA infection revealed numerous leukocytes. Pathologist review determined these cells to be primarily neutrophils (predominantly bands), along with more densely packed collagenous material (Figure 4D). However, by 12 Hpb with PA M2 infection, increasingly more cellular infiltrates were seen, mainly neutrophils (predominantly bands) and less densely packed collagenous materials (Figure 4E). These data suggest the active recruitment of immune cells into the seroma.

Seroma Cytokine and Chemokine Concentration

To determine how these inflammatory cells are recruited to the seroma, we performed cytokine and chemokine analysis on sera and seroma samples from burned mice with and without PA M2 infection. In addition, seroma samples were collected 12 Hpb. In all cases, cytokine and chemokine levels within the seroma were higher in PA M2-infected mice when compared to noninfected mice. Proinflammatory IL-1β, IL-6, and TNF-α were significantly elevated in the seroma with infection at 12 Hpb (Figure 5A–D). IL-10, an immunosuppressive cytokine, was also elevated at the 12 Hpb time point in the seroma of infected mice (Figure 5E).

Likewise, chemokine concentrations of CXCL10 (IP-10), CXCL1 (KC), CCL2 (MCP-1), CCL3 (MIP-1α), CCL4 (MIP-1β), and CCL5 (RANTES) were elevated in the seroma in comparison to the serum. In each case, infected mice had higher levels of IP-10, MCP-1, MIP-1α, MIP-1β when compared to uninfected mice (Figure 6A–E). These data suggest that active recruitment of monocytes and PMN's to the seroma during infection is secondary to the production of chemokines.

Cellular Profile of the Blood and Seroma Postburn

We employed flow cytometry and cell phenotyping to profile the cell types present within the seroma (Supplementary Table 1). At 12 Hpb, whole blood and seroma fluid

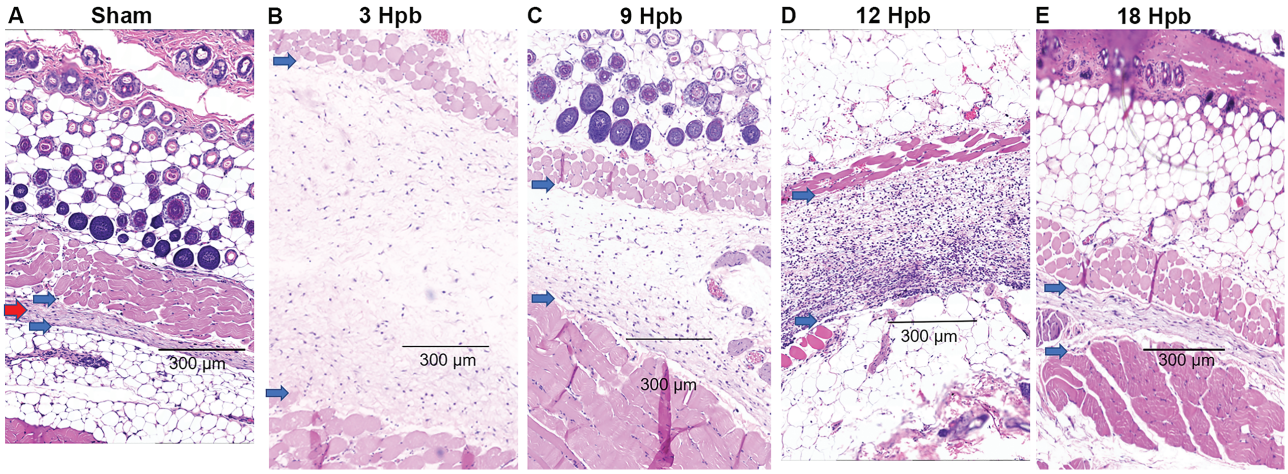

Figure 3. H&E staining of seroma over 18 hours: (A) Subcutaneous fascial plane in unburned skin averages a depth of 57 µm (red arrow). Blue arrows designate the boundaries between the panniculus carnosus and the skeletal muscle/adipose tissue. (B) 3 Hpb, fascial plane increased to an average thickness of 1.18×10^3 µm. (C) 9 Hpb, the average thickness was 1.15×10^3 µm. (D) At 12 Hpb, the average thickness reduced to 567 µm. As the seroma condenses, a large influx of cells was seen filling the area. (E) At 18 Hpb, the fluid layer was reduced to <200 µm. Scale bars are 300 µm.

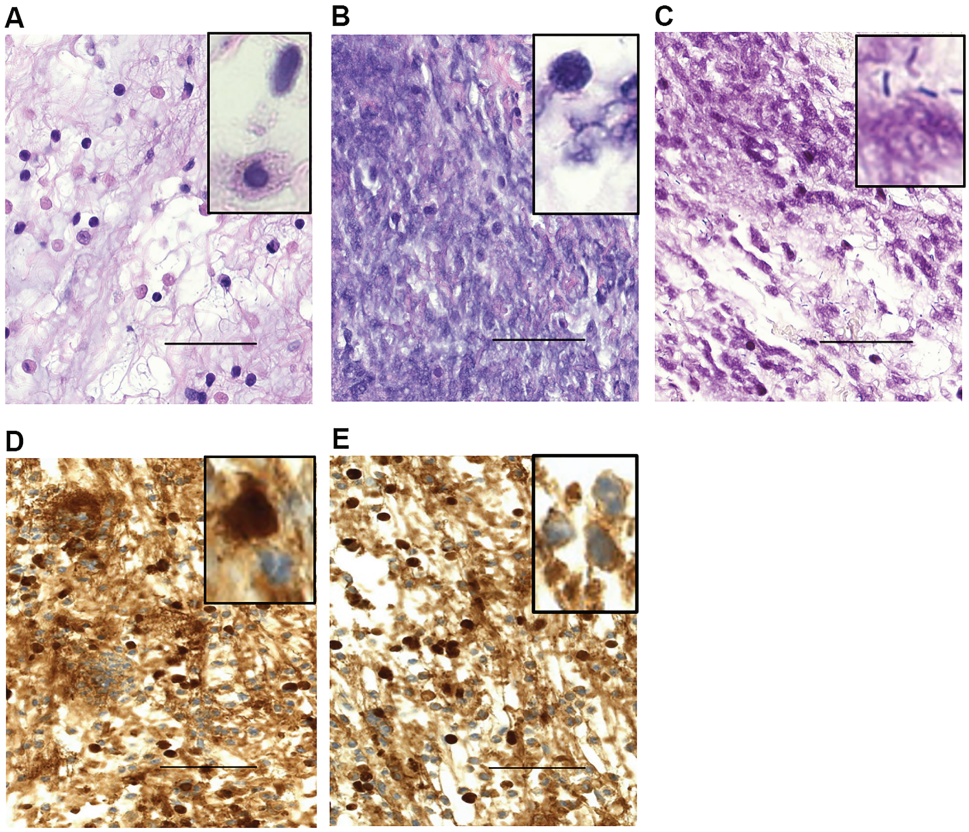

Figure 4. Histological examination of Histogel seroma sections: (A) H&E stain, 12 Hpb without infection, mainly fibroblasts with rare lymphocytes. (B) H&E stain, 12Hpb with s.c. PA M2 infection, similar to (A) but increased cellular necrosis. (C) Gram stain, 12 Hpb with s.c. PA M2 infection showed GNR throughout and in proximity to PMNs. (D) IHC, 12 Hpb without infection CD45 staining shows mainly PMNs (bands) with more densely packed collagenous material. (E) CD45 IHC, 12 Hpb with s.c. PA M2 infection, many more PMNs (bands) with less packed collagenous material. Scale bars are 50 µm, and all images are at 600× with oil emersion.

were collected from burned mice with and without PA M2-infection. Only whole blood was collected from sham mice. Recovered cells from the circulation of sham-treated mice averaged 10.1 × 10^6 cells/mL. Circulating cells of burned mice infected with PA M2 12 Hpb averaged 2.3 × 10^6 cells/mL, and the seroma content was 16.0 × 10^6 cells/g (Supplementary Figure 3). Complete blood count (CBC) with differential showed a transient shift in the ratio of neutrophils to lymphocytes ratio from 0.16 to a peak of 0.57, at 12 hours, which returned to 0.17 after 72 hours in the absence of infection (Supplementary Table 2). We performed flow cytometry on seroma samples postburn at 12 hours with and without infection to profile the CD 45+ cellular content of the seroma. Gating strategies for flow cytometry are shown (Supplementary Figure 4). Primarily two cell types were detected: neutrophils (CD11b+, Ly6G+) and macrophages (CD11b+ F4-80+). Neutrophils made up 94.3% of CD45+ populations in the seroma fluid; macrophages accounted for only 3.3% of all CD45+ cells within the seroma (Figure 7). As neutrophils were the dominant cell type, they were further classified by surface markers Ly6G and CD62L to assess activation, recruitment, and function.[19] Postburn neutrophils showed increased expression of Ly6G in the seroma in both infected and noninfected burned mice compared to circulating neutrophils, suggesting increased activation. Ly6G expression was highest in the seroma of infected burned mice (Figure 8A). The surface expression of CD11b was elevated in the seroma of both noninfected and infected mice; however, their CD11b surface expression in the circulation of all groups remained consistent (Figure 8B). With infection, CD62L surface expression in the seroma neutrophils at 12 Hpb was reduced to almost undetectable levels, suggesting an immature state and that the neutrophils have reached their point of migration (Figure 8C). These data suggest that immature neutrophils were recruited to and stimulated in the seroma regardless of infection. However, neutrophils that reach the seroma, which included viable PA M2, were activated, demonstrated by their near-complete loss of CD62L. Additionally, it is likely these neutrophils are actively recruited to the seroma and are not passively entering the seroma based on the absence of red blood cells.

DISCUSSION

Postburn sepsis continues to be a leading complication for severe burn survivors.[20] Our nonlethal 10% (TBSA) flame burn of outbred CD1 mice allows for dissociation of events caused by the burn itself and the events caused by complications from a superimposed bacterial infection.[17] Following a burn, necropsy revealed a large seroma between the panniculus

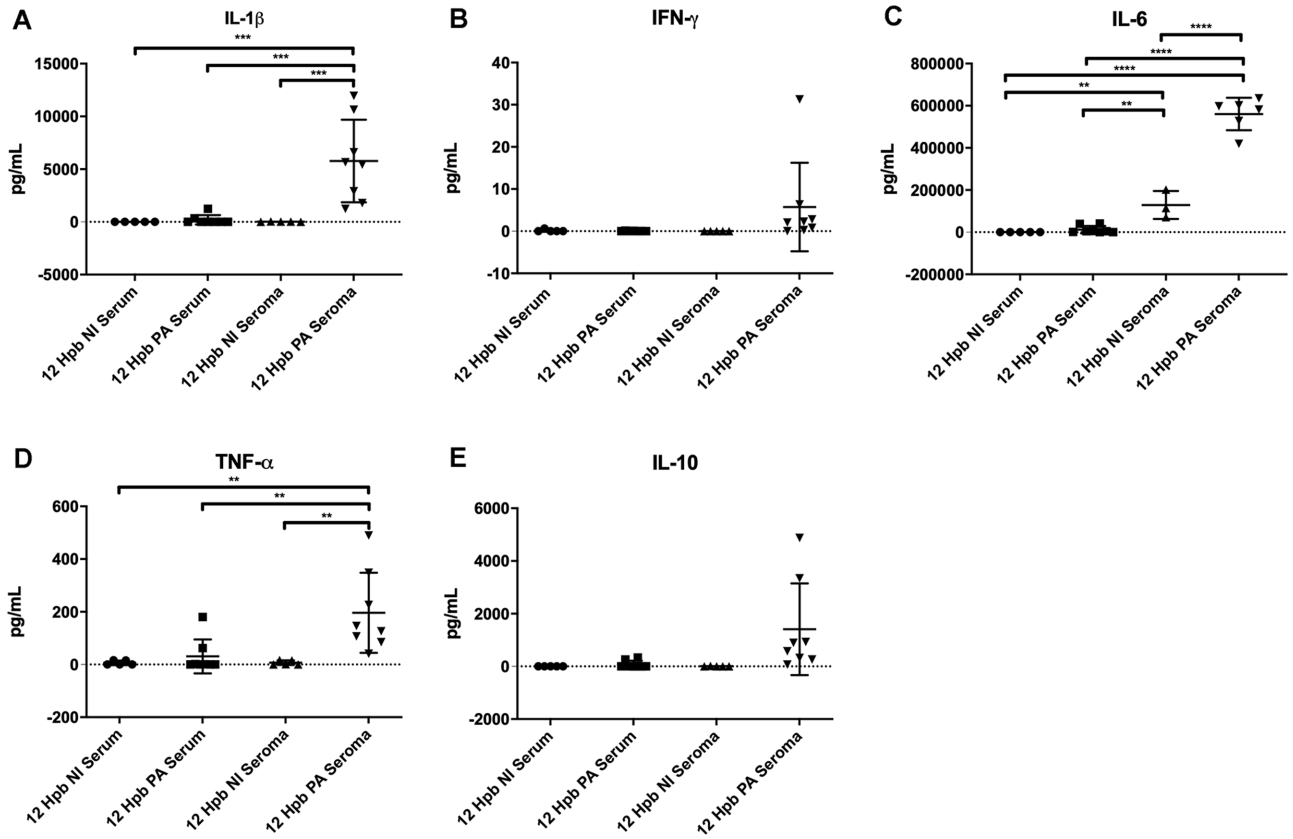

Figure 5. Cytokine concentrations in the serum and seroma with (PA) and without (NI) infection: (A) IL-1B, (B) IFN-γ, (C) IL-6, (D) TNF-α, and (E) IL-10. One way ANOVA with Tukey's multiple comparisons test was used to analyze chemokine concentrations. *$P < .05$, **$P < .01$, ***$P < .001$, ****$P < .0001$.

carnosus and the underlying skeletal muscle. This fluid formation was observed in mice that received either a superimposed subcutaneous infection with PA M2 or no infection postburn. The seroma was estimated to be ~500 µL in volume (~25% of the fluid volume within the circulation) and was completely translucent and gelatinous in texture when separated from the surrounding tissue. The fluid supported the in vitro growth of multiple strains of PA at a rate equivalent to that in fortified bacterial culture media. The seroma was reabsorbed in the absence of infection, as the the increased susceptibility to PA M2 sepsis waned.[17] Histological analysis showed leukocyte infiltrates regardless of infection; with infection, massive cellular necrosis was observed. Local cytokine and chemokine concentrations were elevated in the seroma before appearing in the circulation, and leukocyte recruitment was evident by 12 Hpb. The fluid extended beyond the burn boundaries, suggesting low restriction, the opposite effect of intercompartmental sepsis, an unusual complication of burns in humans.[11,21] (Figure 1). Additionally, i.v. administration of FITC-dextran revealed that the fluid contained in the seroma was derived from the circulation Hpb (Supplementary Figure 1). At 12 hours, we showed by flow cytometry that neutrophils were the prominent CD 45+ cell recruited to the seroma, with a small percentage of macrophages. Neutrophils within the seroma showed a reduced surface expression of CD62L and an increased surface expression of Ly6G, suggesting active recruitment to the seroma.

We chose to classify this as a seroma and not edema, as fluid buildup was only seen between the skeletal muscle and the panniculus carnosus and not within any other tissues. Our histological analysis concurs with that of a skin flap seroma mouse model[22] l. Additionally, the fluid alone was capable of supporting PA growth. PA is a critical opportunistic pathogen that colonizes and infects postsurgical seromas and burn wounds.[15,23] This seroma was short-lived and, in all noninfected mice, receded at a rate correlating with decreased susceptibility to PA-mediated mortality.[17] The seroma reached a maximum expansion at 3 Hpb, and cellular infiltrates were seen by 12 Hpb (Figure 3). IHC and flow cytometry analysis showed that the cellular infiltrates were primarily CD45+ cells indicating immune cell recruitment. Red blood cells were not detected in any of the seroma samples. These data suggest active recruitment of leukocytes into the seroma following the burn and not from a breakdown of vascular endothelium (Figure 4).

Our data suggest that monocytes and PMN's were actively recruited to the seroma by proinflammatory cytokines IL-1β, TNF-α, and IL-6 (Figure 5). Additionally, chemokines such as CXCL10 (IP-10), CCL2 (MCP-1), CCL3 (MIP-1α), and CCL4 (MIP-1β) were elevated in the seroma before the serum (Figure 6). Together, these data demonstrate an environment that is supportive of monocyte and PMN recruitment. Furthermore, CBC with differential cell counts showed an increased ratio of neutrophils to lymphocytes at 12 Hpb, an

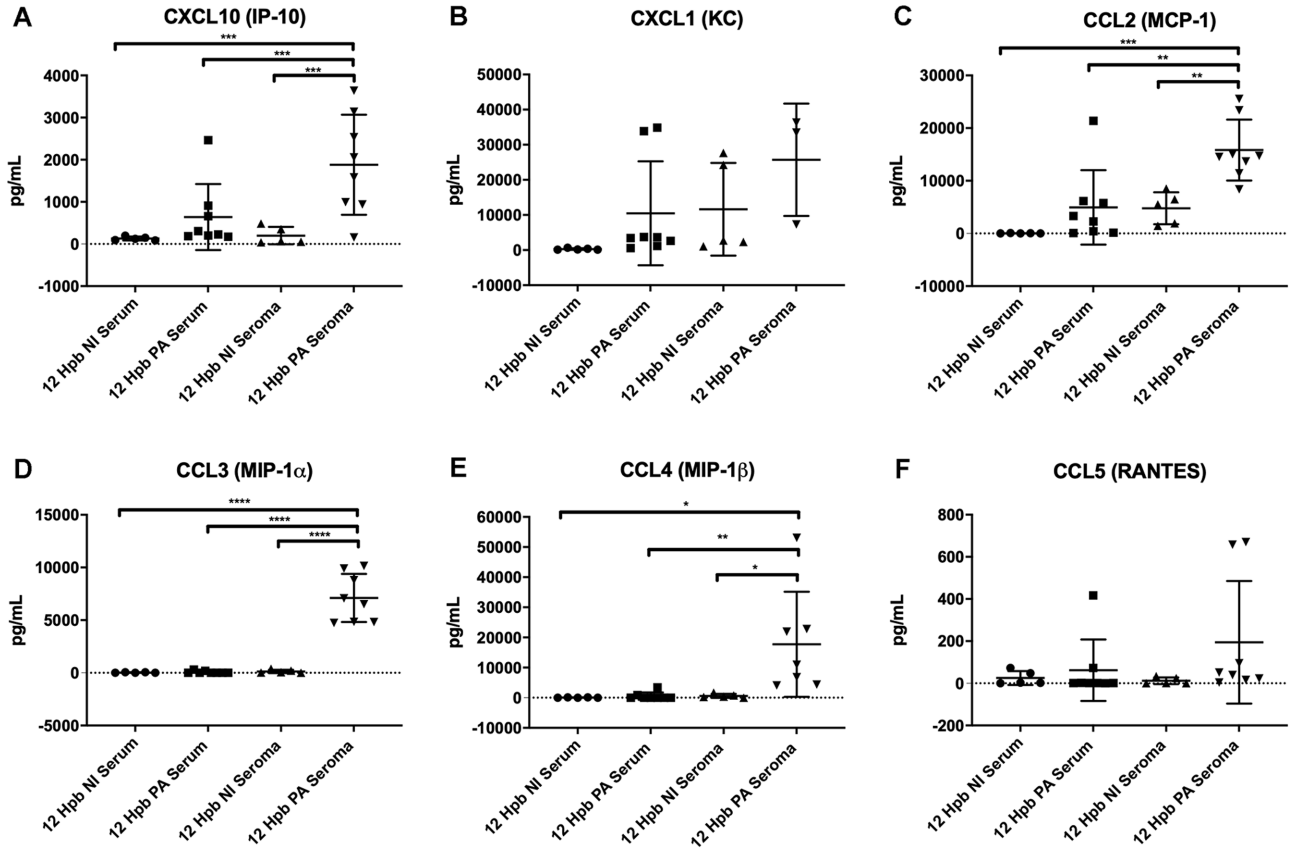

Figure 6. Chemokine concentrations in the serum and seroma with (PA) and without (NI) infection: (A) IP-10, (B) KC, (C) MCP-1, (D) MIP-1α, (E) MIP-1β, and (F) RANTES. One way ANOVA with Tukey's multiple comparisons test was used to analyze chemokine concentrations. **P* < .05, ***P* < .01, ****P* < .001, *****P* < .0001.

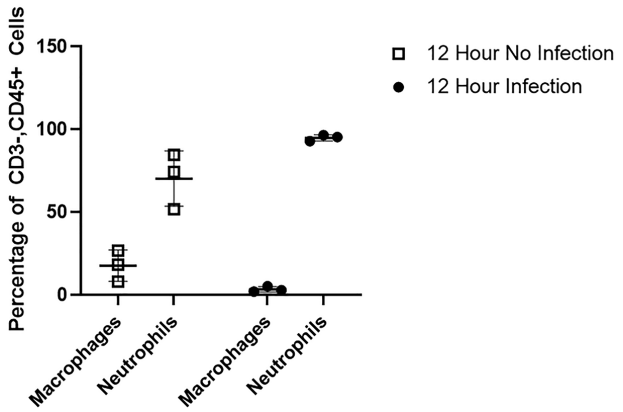

Figure 7. Immune cell populations in the seroma: Percentage of macrophages and neutrophils in the seroma, with and without PA M2 infection (n = 3, per group).

indicator of increased risk of sepsis (Supplementary Table 2).[24] Therefore, cells may be directed to the seroma from the circulation instead of vital organs resulting in a reduction in host defenses at a critical time during infection.

Using flow cytometry, we employed an immune phenotyping panel on cells harvested from the seroma and the blood to determine cellular infiltrates' cell population. CD45+ gating of the seroma revealed that neutrophils and macrophages were in abundance (Supplementary Figure 4). With >90% of the recruited cells being neutrophils in PA M2-infected mice by 12 Hpb. We focused on Ly6G and CD62L, surface markers associated with activation, recruitment, and function.[19] Ly6G surface expression measured by geometric mean fluorescence intensity (gMFI) on neutrophils was high in the seroma of PA-infected mice postburn compared to neutrophils in noninfected burned mice and the circulation of sham mice suggesting an activated state. In addition, CD11b surface expression increased on neutrophils once they entered the seroma regardless of infection, which means that entering the seroma was sufficient to stimulate and prime neutrophils. When in the presence of infecting PA M2, these stimulated neutrophils almost completely lacked CD62L surface expression, indicating they were now activated at the point of recruitment.[25,26] Additionally, histological analysis showed toxic granulation from granulocytes within the seroma and many GNRs near PMN. However, as observed in Gram stains, the bacteria continued to multiply and were not seen inside the PMN, suggesting the neutrophils, although activated, must have been in a dysfunctional state.

To our knowledge, this is the first report of a nonlethal flame-burn murine model that consistently forms a sub-eschar seroma, even in the absence of infection, which appears to have a critical function in the development of PA-mediated sepsis postburn. With a superimposed infection, the seroma served as a proliferation reservoir for PA beyond that which infects

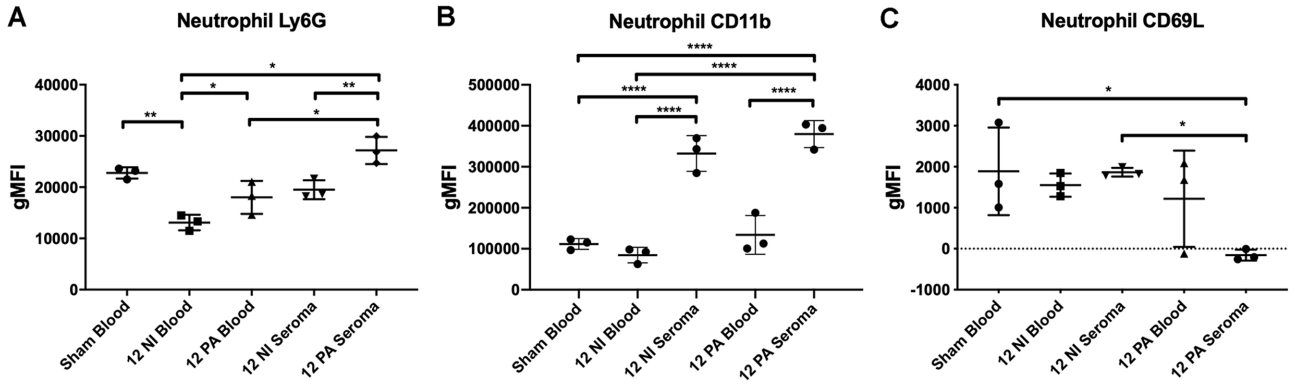

Figure 8. Seroma neutrophil recruitment and activation at 12 Hpb with (PA) and without (NI) infection: gMFI of (A) Ly6G, (B) CD11b, (C) CD62L of neutrophils from blood and seroma of sham, burned + PA M2, and burn without infections. One way ANOVA with Tukey's multiple comparisons test was used to analyze chemokine concentrations. *$P < .05$, **$P < .01$. (n = 3, per group).

the skin surface. Leukocytes, including a large population of immature (bands) and activated neutrophils, were actively recruited to the seroma, which may reduce the availability of these critical immune cells to fight the spreading PA infection in other tissues. No red blood cells were observed within the seroma, suggesting a breakdown of the vascular endothelium was unlikely and that the immune cells were recruited to the seroma and not passively transferred. Gram-negative bacteria were seen near but not within PMNs, suggesting recruited PMNs in the seroma are dysfunctional, despite expressing activation markers.

Additionally, all of these events occur before the onset of clinical symptoms of moribundity. This seroma may be readily visible in mice due to the anatomical structure of mouse skin and the two adjacent muscle layers of the skeletal muscle and the panniculus carnosus. It is likely that seroma formations occur in humans but are not observed. Further investigation of the formation and function of the seroma is critical to understanding the increased susceptibility to PA-mediated sepsis postburn.

SUPPLEMENTARY DATA

Supplementary data is available at *Journal of Burn Care & Research* online.

ACKNOWLEDGEMENTS

We would like to thank Drs. Turhan Coksaygan, Steven Codero, and Novea Simper for their assistance in pathological review. This work would not have been achieved without the assistance of the University of Maryland Center for Innovative Biomedical Resources, Pathology Biorepository Shared Services and Cytokine Core Laboratories, and their dedicated staff of Ashley Cellini, Kimberly Clark, and Lisa Hester.

REFERENCES

1. Organization WH. Burns fact sheet. 2018. Available from: https://www.who.int/news-room/fact-sheets/detail/burns; accessed 6 March 2018.
2. Alp E, Coruh A, Gunay GK, Yontar Y, Doganay M. Risk factors for nosocomial infection and mortality in burn patients: 10 years of experience at a university hospital. J Burn Care Res 2012;33:379–85.
3. Peck MD. Epidemiology of burns throughout the world. Part I: distribution and risk factors. Burns 2011;37:1087–100.
4. American Burn Association. Burn incidence fact sheet. Available from: https://ameriburn.org/who-we-are/media/burn-incidence-fact-sheet/
5. Pham TN, Cancio LC, Gibran NS; American Burn Association. American Burn Association practice guidelines burn shock resuscitation. J Burn Care Res 2008;29:257–66.
6. Foster K. Clinical guidelines in the management of burn injury: a review and recommendations from the organization and delivery of burn care committee. J Burn Care Res 2014;35:271–83.
7. Orgill DP, Piccolo N. Escharotomy and decompressive therapies in burns. J Burn Care Res 2009;30:759–68.
8. D'Avignon LC, Saffle JR, Chung KK, Cancio LC. Prevention and management of infections associated with burns in the combat casualty. J Trauma 2008;64(3 Suppl):S277–86.
9. Pruitt BA Jr. Protection from excessive resuscitation: "pushing the pendulum back". J Trauma 2000;49:567–8.
10. Sheridan RL, Tompkins RG, McManus WF, Pruitt BA Jr. Intracompartmental sepsis in burn patients. J Trauma 1994;36:301–5.
11. Chou C, Lee SS, Wang HM et al. Intracompartmental sepsis with burn: a case report. Ann Plast Surg 2016;76 Suppl 1:S25–8.
12. Dyess DL, Ferrara JJ, Luterman A, Curreri PW. Subeschar tissue fluid: a source of cell-mediated immune suppression in victims of severe thermal injury. J Burn Care Rehabil 1991;12:101–5.
13. Ferrara JJ, Dyess DL, Luterman A, Curreri PW. The suppressive effect of subeschar tissue fluid upon *in vitro* cell-mediated immunologic function. J Burn Care Rehabil 1988;9:584–8.
14. Singh A, Anand A, Mittal S, Sonkar AA. Morel-Lavallee seroma (post-traumatic pseudocyst) of back: a rarity with management conundrum. BMJ Case Rep 2016;2016. Epub 2016/07/21. doi: 10.1136/bcr-2016–216122. PubMed PMID: 27435850; PMCID: PMC4964255.
15. Axelsson CK, Qvamme GM, Okholm M et al. Bacterial colonization of seromas after breast cancer surgery with and without local steroid prophylaxis. World J Surg Oncol 2019;17:120.
16. Stieritz DD, Holder IA. Experimental studies of the pathogenesis of infections due to *Pseudomonas aeruginosa*: description of a burned mouse model. J Infect Dis 1975;131:688–91.
17. Brammer J, Choi M, Baliban SM et al. A non-lethal murine flame burn model leads to a transient reduction in host defenses and enhanced susceptibility to lethal *Pseudomonas aeruginosa* infection. Infect Immun 2021;89:e0009121. Epub 2021/06/22. doi: 10.1128/IAI.00091-21. PubMed PMID: 34152806.
18. Ullman-Culleré MH, Foltz CJ. Body condition scoring: a rapid and accurate method for assessing health status in mice. Lab Anim Sci 1999;49:319–23.
19. Lee PY, Wang JX, Parisini E, Dascher CC, Nigrovic PA. Ly6 family proteins in neutrophil biology. J Leukoc Biol 2013;94:585–94.
20. Zhang P, Zou B, Liou YC, Huang C. The pathogenesis and diagnosis of sepsis post burn injury. Burns Trauma 2021;9:tkaa047.
21. Peñuelas O, Cerdá E, Espino J et al. Limb intracompartmental sepsis in burn patients associated with occult infection. Burns 2010;36:558–64. Epub 2009/10/09. doi: 10.1016/j.burns.2009.06.201. PubMed PMID: 19819076.
22. Huang H, Kong D, Liu Y et al. Sapylin promotes wound healing in mouse skin flaps. Am J Transl Res 2017;9:3017–26.

23. Azzopardi EA, Azzopardi E, Camilleri L et al. Gram negative wound infection in hospitalised adult burn patients–systematic review and metanalysis. PLoS One 2014;9:e95042.
24. Hwang SY, Shin TG, Jo IJ et al. Neutrophil-to-lymphocyte ratio as a prognostic marker in critically-ill septic patients. Am J Emerg Med 2017;35:234–9.
25. Stockfelt M, Christenson K, Andersson A et al. Increased CD11b and decreased CD62L in blood and airway neutrophils from long-term smokers with and without COPD. J Innate Immun 2020;12:480–9.
26. Kuhns DB, Long Priel DA, Gallin JI. Loss of L-selectin (CD62L) on human neutrophils following exudation in vivo. Cell Immunol 1995;164:306–10.